Journal of Atmospheric and Solar-Terrestrial Physics 89 (2012) 27–32

Contents lists available at SciVerse ScienceDirect

Journal of Atmospheric and Solar-Terrestrial Physics

journal homepage: www.elsevier.com/locate/jastp

Short Communication

An unusual reduction in the mesospheric semi-diurnal tidal amplitude over Tirunelveli (8.7°N, 77.8°E) prior to the 2011 minor warming and its relationship with stratospheric ozone

S. Sridharan [a,*], S. Sathishkumar [b], S. Gurubaran [b]

[a] *National Atmospheric Research Laboratory, Gadanki 517112, India*
[b] *Equatorial Geophysical Research Laboratory, Indian Institute of Geomagnetism, Krishnapuram, Tirunelveli 627011, India*

ARTICLE INFO

Article history:
Received 10 May 2012
Received in revised form
17 July 2012
Accepted 25 July 2012
Available online 8 August 2012

Keywords:
Stratospheric sudden warming
Ozone
Mesospheric tides
Brewer–Dobson circulation

ABSTRACT

There is an unusual decrease of semi-diurnal tidal amplitude in zonal wind at 88 km over Tirunelveli (8.7°N, 77.8°E) prior to the onset of a minor warming event of 2011. During that time, there is a sudden decrease of TIMED-SABER observed ozone volume mixing ratio (VMR) at equator and 60°N. It is suggested that the enhanced planetary wave activity prior to the occurrence of SSW increases the strength of the Brewer–Dobson circulation, which transports stratospheric ozone, the solar insolation absorption of which mainly generates semi-diurnal tide, to high-latitude lower stratosphere and as expected, ozone VMR at 70°N increases in the lower stratosphere.

1. Introduction

In the winter polar stratosphere, stratospheric sudden warming (SSW) occurs as a result of the interactions between vertically propagating planetary waves and the zonal winds (McIntyre, 1982). The tidal variabilities at high-latitudes have been reported in the past in a few studies in relation with the SSW events (Bhattacharya et al., 2004; Hoffmann et al., 2007; Jacobi et al., 1999). At equatorial and low-latitudes also, recent studies have shown enhanced semi-diurnal variations in mesospheric winds (Sridharan et al., 2009), vertical plasma drifts (Chau et al., 2009), total electron content (TEC) (Goncharenko et al., 2010) and N_mF_2 and h_mF_2 (Yue et al., 2010). It is found that the ozone mixing ratio increases at low-latitudes during the SSW due to reduced planetary wave activity during the SSW event, which may prevent the transport of ozone from low to high latitudes (Sridharan et al., 2012). As semi-diurnal tide is produced due to solar insolation absorption of ozone, the increase in the ozone mixing ratio could be a reason for the increase in the semi-diurnal tidal amplitude.

Fejer et al. (2011) observed the time of maximum downward perturbation in the vertical plasma drifts over Jicamarca becomes later on succeeding days and indicated the influence of lunar tides. Recently Stening (2011) suggested that the changes observed at low-latitudes are mostly due to lunar tides and the circulation changes due to SSW favors the vertical propagation of lunar tides to reach ionospheric heights. Pedatella and Forbes (2010) showed that migrating semidiurnal tide of zonal wave-number 2 in Global Ionospheric Maps (GIMs) of GPS TEC has a 14 day periodicity in its amplitude at the anomaly crests, which suggests a lunar effect persisting from January to March 2009. However, it may be noted that ~16-day planetary wave was dominant during that period (Sridharan et al., 2009) and ~14-day periodicity may be due to the modulation of the tide by the planetary wave. Stening et al. (1996) suggested the possibility that counter-electrojets (CEJs) might be due to a lunar atmospheric semidiurnal tide since the vertical propagation of such a tide may be enhanced during the atmospheric conditions associated with an SSW. They found that 15 out of the 23 events occurred near to full moon or new moon.

It is important to investigate with more cases whether the relationship between SSW and low-latitude tidal variabilities is just coincident or not. Recent minor warming of 2011 has given an opportunity to study the relationship between variabilities of tides at low-latitudes and the SSW.

2. Data analysis

2.1. MF radar at Tirunelveli

The MF radar at Tirunelveli (8.7°N, 77.8°E) is operating at 1.98 MHz and it has been giving horizontal wind information in the upper mesospheric region (78–98 km) with 2-min time

* Corresponding author. Tel.: +91 8585 272124; fax: +91 8585 27 2018.
E-mail addresses: SuSridharan@narl.gov.in, ssri_dhar@rediffmail.com (S. Sridharan).

1364-6826/$ - see front matter © 2012 Elsevier Ltd. All rights reserved.
http://dx.doi.org/10.1016/j.jastp.2012.07.012

resolution since November 1992 (Rajaram and Gurubaran, 1998). The 2 min sampled wind measurements are averaged for each hour and used for tidal analysis. The rate of data acceptance, which is based on several data rejection criteria (Briggs, 1984), is higher only above 84 km altitude. Besides, radar tends to measure electron drift motion rather than neutral winds at altitudes above 92 km (Gurubaran and Rajaram, 2000). Hence, for the present study, the tidal amplitudes are computed for zonal winds at 88 km using a least squares harmonic fit with mean and tidal components of periods 24 h, 12 h and 8 h over a five-day composite window of hourly wind values, which is successively forwarded every day to obtain the daily variation of tidal components. The five-day window is chosen so that it will average out all incoherent wind variations mostly due to gravity waves.

2.2. ERA-interim data

In this paper, we use a few ERA-interim zonal wind and temperature available for the 37 pressure levels from the surface to 1 hPa at the ECMWF (European Center for Medium Range Weather Forecasting) website (www.ecmwf.int/research/era/do/get/index). These data were prepared by ECMWF using their variational data assimilation system (Berrisford et al., 2009). The ERA-interim data set consists of results from analysis conducted at 6-h intervals available for a 1.5° latitude–longitude grid.

2.3. TIMED-SABER ozone observations

The SABER instrument is basically a multi-channel radiometer, which views limb of Earth atmosphere's and measures near to mid-infrared emissions over the range 1.27–17 μm (7865–650 cm^{-1}) corresponding to the line-of-sight tangent point, which are used to retrieve the kinetic temperature and mixing ratios of several minor constituents. Measurements are made over the globe from about 100 hPa to altitudes higher than 0.001 hPa (~16 to 96 km), over 24 h in local solar time, since the beginning of 2002. The present study utilizes version 1.07 of processed level 2 ozone volume mixing ratio (VMR) data available in the website http://saber.gats-inc.com/. The SABER uses 1.27 μm emissions from molecular oxygen and the strong 9.6 μm emission from ozone itself, to obtain ozone profiles (Smith et al., 2009). As the origin of 9.6 μm emission is thermal in nature, observations are made during both day and night using this emission. The zonal mean ozone measurements at 9.6 μm are used in the present study.

3. Results

Fig. 1 shows daily variation of amplitude of planetary wave (PW) of zonal wave number (k) 1 and 2 in temperature at 10 hPa and temperature difference between 90°N and 60°N at 10 hPa for the day numbers 1–59 starting from January 01, 2011. It may be noted that the amplitude of PW of $k=1$ is generally larger than that of $k=2$ during January–February 2011, and it undergoes large variabilities with maximum amplitude around the day numbers 4, 15 and 28. The temperature difference between the latitudes 90°N and 60°N also shows similar variabilities. However, only the third larger maximum in the PW amplitude and its subsequent decrease are accompanied by positive polar temperature difference between the latitudes 90°N and 60°N during the day numbers 31–35. The maximum polar temperature difference between the latitudes 90°N and 60°N is observed to be 15 K. Though the decrease of PW is noted from day number 30, it drastically decreases on day number 34. Due to transient nature of the wave, it interacts with the mean flow and provides westward acceleration. As a result, the mean zonal wind at 60°N at 10 hPa shows deceleration and attains the eastward wind speed of ~25 m/s on day number 34. The deceleration does not give rise to reversal of zonal wind, as the polar vortex is too strong during this winter leading to unprecedented ozone loss (Manney et al., 2011). As the mean zonal mean wind at 60°N does not show any reversal to westward wind, it is considered only as a minor warming. Recent major warming event occurred in the year 2009 with the maximum polar temperature difference of ~25 K

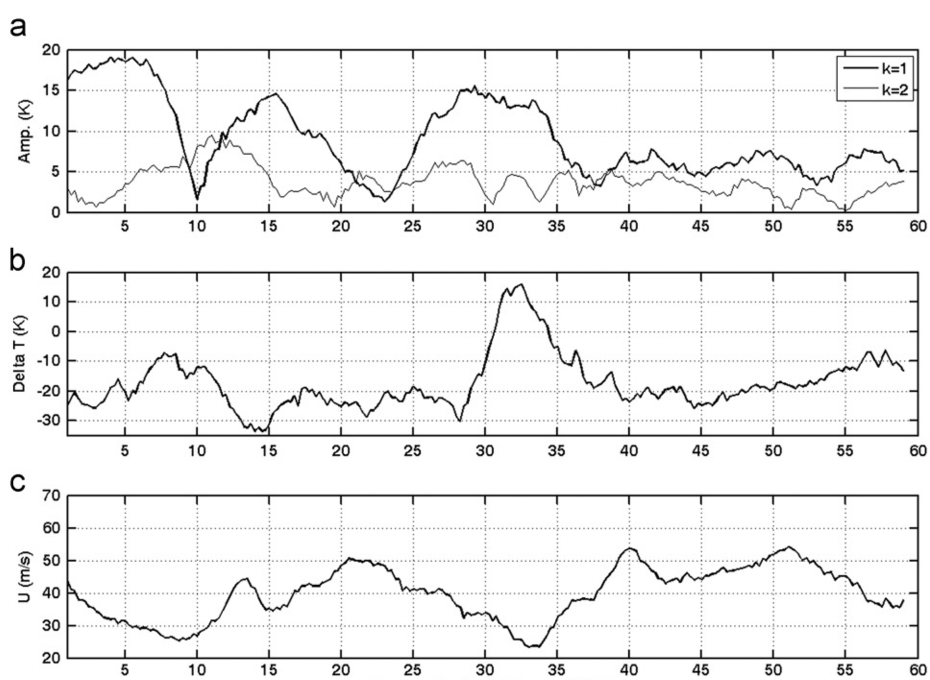

Fig. 1. (a) Daily variation of planetary wave amplitude of zonal wavenumbers 1 and 2 at 10 hPa, (b) zonal mean temperature difference at 10 hPa between the latitudes 90°N and 60°N, and (c) zonal mean zonal wind at 60°N and at 10 hPa.

associated with the unprecedented reversal of eastward wind to westward wind of magnitude ~50 m/s.

Sridharan et al. (2009) found enhanced mesospheric semi-diurnal tidal amplitude over a low-latitude site, Tirunelveli (8.7°N, 77.8°E) during the major SSW of 2009. It is interesting to see the tidal variabilities during the minor SSW of 2011. The diurnal (24 h), semi-diurnal (12 h) and ter-diurnal (8 h) tidal amplitudes and phases at 88 km are shown in Fig. 2. It may be noted that there is an unusual reduction in the semi-diurnal tidal amplitude during day numbers 26–33, when the amplitude is less than 6 m/s. On days 30–32, the amplitude is around and even less than 2 m/s, just before the onset of minor warming. After the minor warming, there is a large enhancement in the diurnal tidal amplitude on day number 37. The diurnal tidal amplitudes are greater than 10 m/s on most of the days. The phase of the semi-diurnal tide does not show any remarkable day-to-day variation. However, the diurnal tide shows that its phase advances slowly to early hours, as day progresses during day numbers 20–35. The ter-diurnal tidal amplitude does not show any remarkable variation in relation with the SSW event. This is in contrast to the recent numerical simulations (Fuller-Rowell et al., 2011; Wang et al., 2011) which predict an increase in the ter-diurnal tide due to SSW event and a decrease in the amplitude of the semi-diurnal tide.

Recently, Sridharan et al. (2012) observed an ozone enhancement in the tropics during the major SSW event of 2009 and suggested that it could be a reason for the enhancement in the amplitude of semi-diurnal tide, which is mainly generated due to absorption of solar radiation by ozone. The height–time cross section of ozone volume mixing ratio is shown in Fig. 3 for day numbers 1–59, 2011 and for the heights 20–45 km over the equator and 60°N. It is clear that the ozone mixing ratio is less in a narrow height region 32–35 km during the day numbers 23–34 over the equator and at a relatively broader height region 32–42 km during day numbers 25–34 at 60°N. However, there is an enhancement in ozone VMR at high latitude stratosphere. The time–height cross section ozone VMR for the heights 20–30 km shows that the ozone mixing ratio is larger during day numbers 23–32 km (greater than 3.5 VMR) in the height region 20–25 km. During day numbers 25–30, the ozone VMR is greater than 4 VMR. The variations in ozone VMR at high latitudes may be due to different processes, namely, development of the polar vortex, advection of ozone, or catalytic ozone destruction (Scheiben et al., 2011). As there is an increase of ozone in the lower stratosphere, more probably the ozone is transported by meridional circulation from low to high latitudes.

As the ozone heating is in the extended altitude region 30–50 km and it is maximizing around 48 km (Xu et al., 2012), it would be of interest to see closely the latitude variation of ozone mixing ratio at different heights. As shown in Fig. 4a–c, the ozone mixing ratio is in general low at mesospheric heights (above 50 km) and at stratospheric heights, it is less for a few days around day number 60 at all latitudes. In particular, at 48 km, where ozone heating is larger, the ozone VMR is greater than 4 ppm during day numbers 16–28, whereas it is less than 4 ppm during day numbers 29–34 at 40°N. At equator, ozone VMR is around 3 ppm during day numbers 25–35 and around 40. At 44 km, a decrease of ozone VMR is noticed at 20°N for the day numbers 20–30. At 40 km, decrease of ozone VMR is clearly observed during day numbers 20–30. Fig. 4d–f shows ozone VMR at 20°N, 10°N and equator averaged for the heights 30–60 km. It clearly shows the presence of less ozone VMR during day numbers 20 and 30 at equator and 10°N. Though semi-diurnal tidal heating due to solar insolation absorption by ozone is larger at 48 km (Groves, 1982), heating rate at 35 km is around 4–5 °C/day, which is nearly 40–50% of maximum heating rate at equator.

The distribution of stratospheric minor constituents, like ozone, is modified by the large-scale circulation, known as the Brewer–Dobson (BD) circulation, consisting of tropical upwelling and high latitude downwelling. Rossby waves are important for the existence of BD circulation (Scott and Polvani, 2004). The intense northern hemisphere waves produce a stronger BD circulation, a weaker polar vortex, and a warmer polar temperature of the polar vortex. Because of the stronger BD circulation,

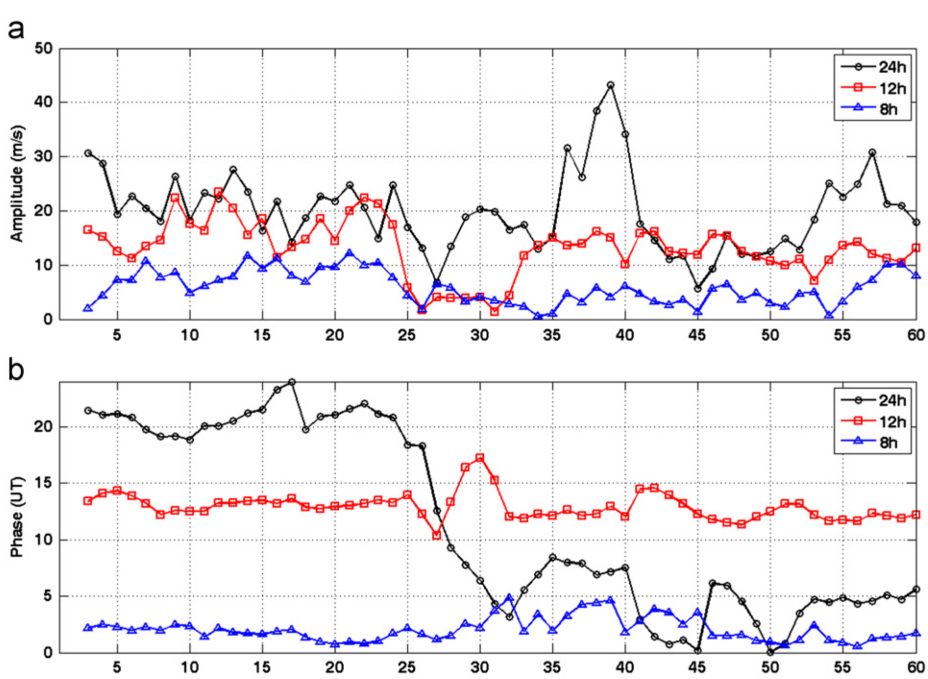

Fig. 2. Daily variation of diurnal, semi-diurnal and ter-diurnal tidal amplitudes (a) and phases (b) in zonal winds at 88 km over Tirunelveli.

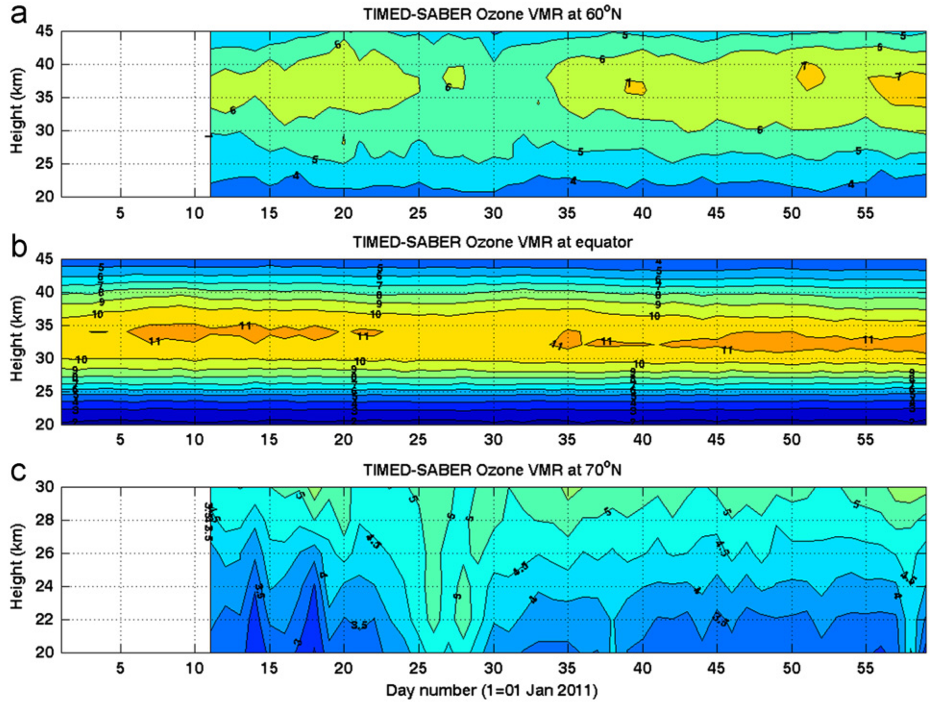

Fig. 3. Time–height cross section of ozone volume mixing ratio (SABER) for (a) 60°N, (b) equator and (c) 70°N.

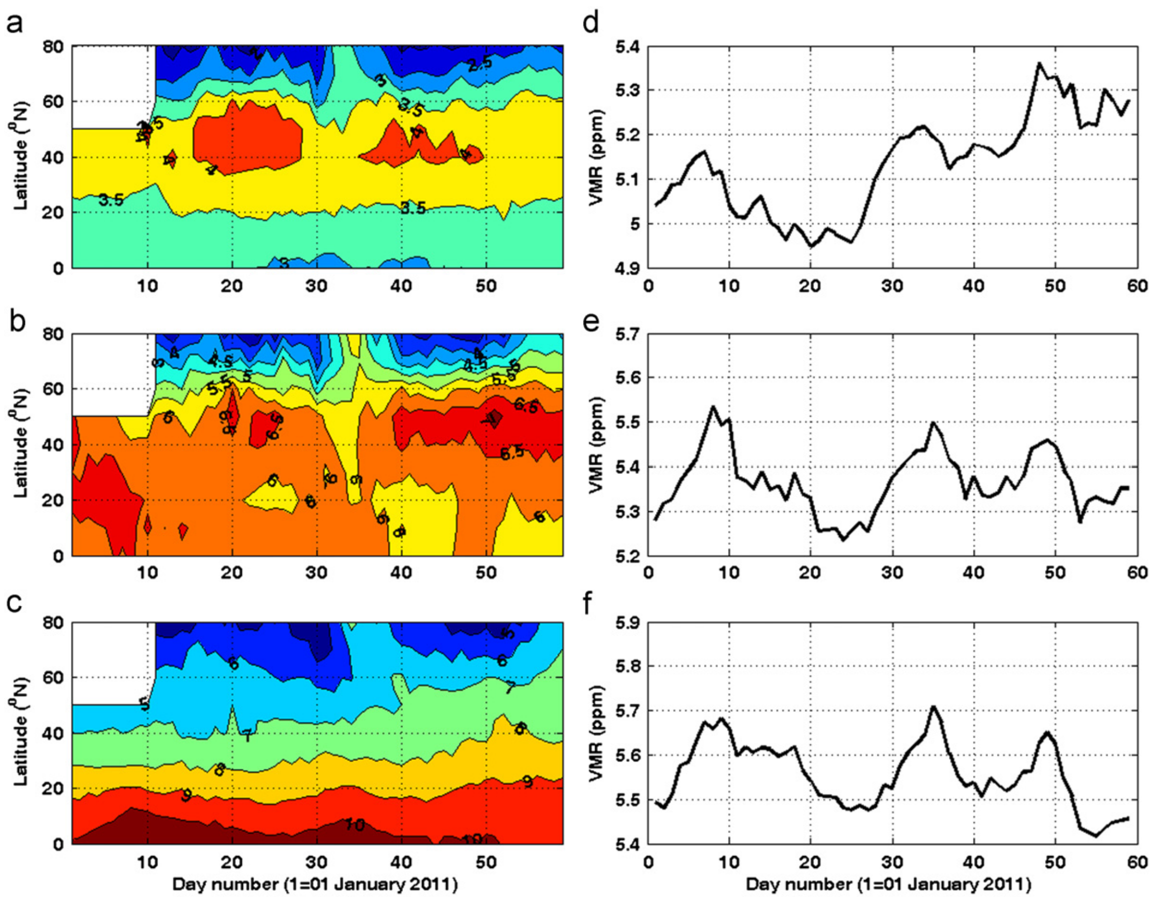

Fig. 4. (a–c) Latitude–time cross section of ozone VMR for the heights 48 km, 44 km and 40 km respectively and (d–f) daily variation of ozone VMR averaged for the altitudes 30–60 km at 20N, 10N and equator respectively.

more ozone is transported to the northern polar lower stratosphere. The BD circulation is approximately represented by the residual circulation (RC) and considered to be driven by the body force induced mainly by the breaking and/or dissipation of the Rossby waves. The residual meridional and vertical velocities are calculated from the following relations using ERA interim

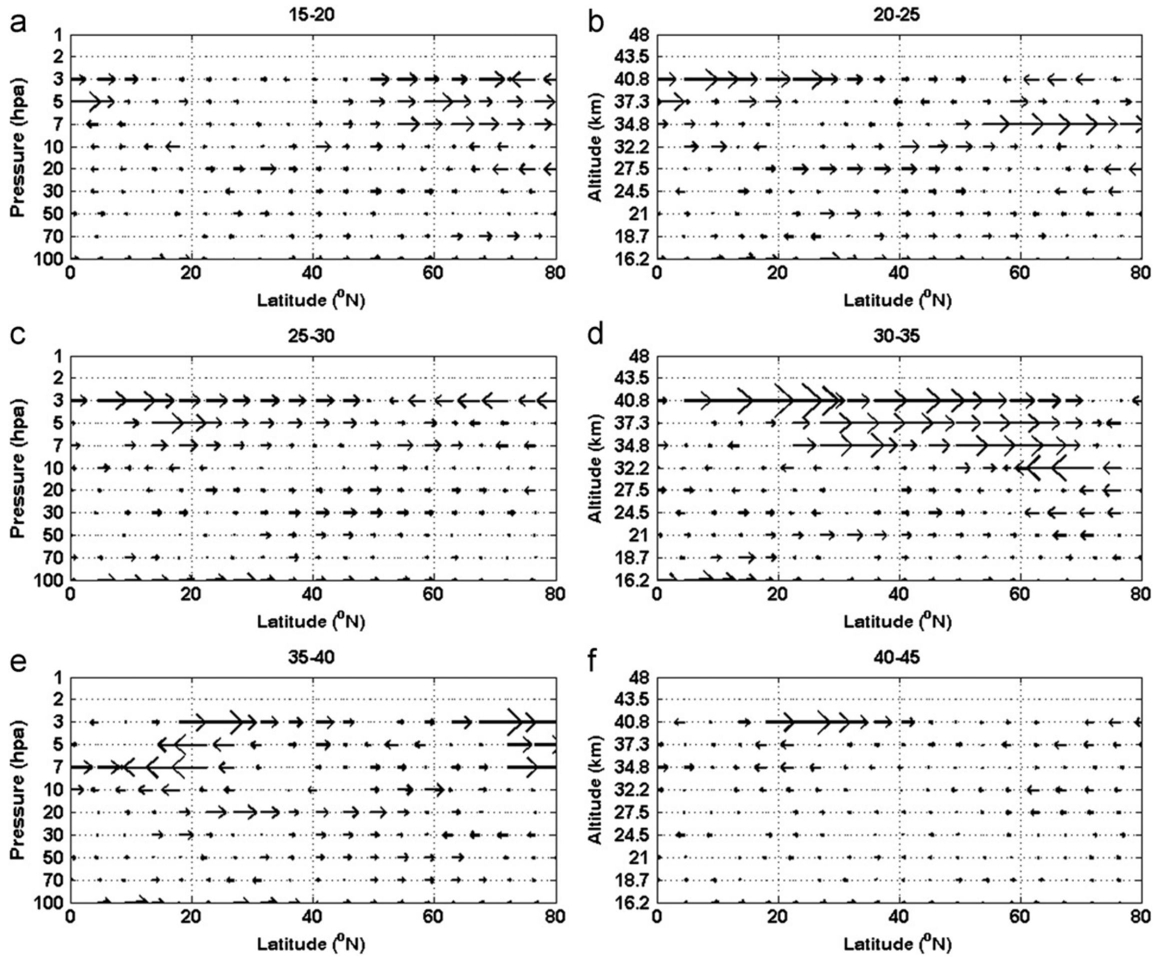

Fig. 5. Residual circulation averaged for day numbers 15–20, 20–25, 25–30, 30–35 and 35–40 of 2011. The vector length calculated from labels of horizontal axis (as vectors are mostly horizontal) is to be multiplied by 0.2 (panel 'a') 0.25 (panels 'b–e') and 0.5 (panel 'f') to get the magnitude of the vector in meter per second. The vertical axis is given in pressure levels for the left panels and in corresponding altitudes for the right panels for reference.

meridional and vertical velocities (Andrews et al., 1987):

$$\overline{v^*} = \overline{v} - \frac{1}{\rho_0}\frac{\partial}{\partial z}(\rho_0 \overline{v'\theta'}/\overline{\theta}_z)$$

$$\overline{w^*} = \overline{w} - \frac{1}{a\cos\varphi}\frac{\partial}{\partial\varphi}(\rho_0 \overline{v'\theta'}/\overline{\theta}_z)$$

The resultant vectors of residual meridional and vertical velocities averaged for the day numbers 10–15, 15–20 and 20–25 are shown as a function of latitude and pressure levels in Fig. 5. It can be seen that the residual circulation (RC) is strongly poleward during day numbers 20–35 at all latitudes above 7 hPa. In particular, during day numbers 20–35, when decrease of ozone mixing ratio is observed at equator, the RC is poleward even from low-latitudes at pressure levels 3–7 hPa. During this period, the diurnal tidal phase shows slow transition toward earlier hours. During day numbers 15–20, the RC is largely poleward above 10 hPa, but it is confined to poleward of 40°N. During day numbers 40–45, the RC becomes equatorward below 5 hPa and continues to be poleward at 3 hPa. It suggests that BD circulation gets weakened due to the decrease of planetary wave activity as a consequence of onset of SSW.

4. Discussion and conclusion

The present study shows an unusual decrease in the semi-diurnal tidal amplitude in zonal wind at 88 km over Tirunelveli just prior to the onset of a minor warming event of 2011. During that time, there is a sudden decrease in the ozone VMR at equator and also at 60°N observed by SABER instrument onboard TIMED satellite. This result is important to demonstrate the relationship between the high latitude northern hemispheric SSW event and low-latitude mesospheric tidal variability through variability in the ozone, as semi-diurnal tide is produced due to solar insolation absorption of ozone and the decrease in the ozone mixing ratio could be a reason for the decrease in the semi-diurnal tidal amplitude.

As the E-region current system is driven by tidal winds, the tidal variabilities during SSW events show remarkable changes in the low-latitude electrodynamics. Occurrence of afternoon counter-electrojet (CEJ) (Sridharan et al., 2009), large semi-diurnal tidal variation in vertical plasma drifts during daytime (Chau et al., 2009), and semi-diurnal variation and large values of total electron content (TEC) (Goncharenko et al., 2010) have recently been reported. Recently, Stening (2011) stressed the importance of lunar tides for the occurrence of CEJ. Fejer et al. (2011) observed the time of maximum downward perturbation in the vertical plasma drifts over Jicamarca becomes later on succeeding days and attributed it as due to the influence of lunar tides. However, the semi-diurnal tidal phases in zonal winds over Tirunelveli do not show any shift to later hours on succeeding days during January–February 2011, shown in Fig. 2 and also during January–February 2009 (not shown), when a major warming event occurred.

Non-linear interaction between tides and planetary waves has been suggested as a potential mechanism for the enhancement of semi-diurnal tide during the warming events (Liu et al., 2010). It can be considered as a potential mechanism, as SSW events are primarily caused by the anomalous growth of planetary waves in the troposphere, their vertical propagation into the stratosphere and their critical level interaction with the background flow. Pancheva et al. (2009) observed enhanced nonmigrating tides associated with nonlinear interaction between migrating tides and stationary planetary waves in the SABER temperatures during the major SSW of 2003/2004. Recently, Pedatella and Forbes (2010) found an increase in both migrating and non-migrating semi-diurnal tidal amplitudes in GPS TEC during SSW events. Different model simulations of non-linear interaction between tides and planetary waves give different results. Decrease of semi-diurnal tide and increase of ter-diurnal tide are noted in the Whole Atmosphere Model (WAM) (Fuller-Rowell et al., 2011), whereas increase of diurnal and semi-diurnal tides are noted in the TIME-GCM model and the maximum increase in the semi-diurnal tide is noted 1 day after the peak in planetary wave activity (Liu et al., 2010). However, our observations show that semi-diurnal tidal amplitudes are enhanced, after the planetary wave activity is decreased (Sathishkumar and Sridharan, 2009; Sridharan et al., 2009, 2012). These results suggest that non-linear interaction may not be a key mechanism for the enhancement of semi-diurnal tidal amplitudes and associated ionospheric disturbances. The enhanced semi-diurnal tidal amplitude, after the decrease of planetary wave activity suggests the weakening of BD circulation, which transport minor constituents like ozone from tropical atmosphere, where it is produced, to high latitudes. This causes accumulation of ozone at low-latitudes. Sridharan et al. (2012) and Goncharenko et al. (2012) found an ozone enhancement in the tropics during the major SSW event of 2009 and suggested that it could be a reason for the amplitude enhancement of semi-diurnal tides, which is mainly generated due to absorption of solar radiation by ozone.

The results of the present study suggest that the enhanced planetary wave activity just prior to the occurrence of SSW increases the strength of BD circulation, which transports ozone produced in the tropics to high latitude lower stratosphere. As expected, the latitude–time cross section of ozone VMR increases in the high latitude lower stratosphere (70°N) during the same period, when the VMR is reduced in the tropical stratosphere. The loss of ozone at low-latitude stratosphere at heights 30–60 km, where the ozone heating is larger, is responsible for the large decrease of semi-diurnal tidal amplitude.

Acknowledgments

The authors acknowledge ECMWF for providing ERA-interim data sets through their website (http:/ecmwf.int/research/era/do/get/index) and TIMED-SABER team for providing ozone VMR through the website http://saber.gats-inc.com/. The authors also acknowledge the CAWSES-India program of ISRO.

References

Andrews, D.G., Holton, J.R., Leovy, C.B., 1987. Middle Atmosphere Dynamics. Academic, San Diego, California 504 pp.

Berrisford, P., Dee, D., Fielding, K., Fuentes, M., Kallberg, P., Kobayashi, S., Uppala, S., 2009. The ERA-interim archive. European Centre for Medium Range Weather Forecasts, Shinfield Park, Reading, Berkshire RG2 9AX, United Kingdom, pp. 1–16.

Bhattacharya, Y., Shepherd, G.G., Brown, S., 2004. Variability of atmospheric winds and waves in the Arctic polar mesosphere during a stratospheric sudden warming. Geophysical Research Letters 31, L23101, http://dx.doi.org/10.1029/2004GL020389.

Chau, J.L., Fejer, B.G., Goncharenko, L.P., 2009. Quiet variability of equatorial ExB drifts during a sudden stratospheric warming event. Geophysical Research Letters 36, L05101, http://dx.doi.org/10.1029/2008GL036785.

Fejer, B.G., Tracy, B.D., Olson, M.E., Chau, J.L., 2011. Enhanced lunar semidiurnal equatorial vertical plasma drifts during sudden stratospheric warmings. Geophysical Research Letters 38, L21104, http://dx.doi.org/10.1029/2011GL049788.

Fuller-Rowell, T., Wang, H., Akmaev, R., Wu, F., Fang, T.-W., Iredell, M., Richmond, A., 2011. Forecasting the dynamic and electrodynamic response to the January 2009 sudden stratospheric warming. Geophysical Research Letters 38, L13102, http://dx.doi.org/10.1029/2011GL047732.

Goncharenko, L.P., Chau, J.L., Liu, H.-L., Coster, A.J., 2010. Unexpected connections between the stratosphere and ionosphere. Geophysical Research Letters 37, L10101, http://dx.doi.org/10.1029/2010GL043125.

Goncharenko, L.P., Coster, A.J., Plumb, R.A., Domeisen, D.I.V., 2012. The potential role of stratosphericozone in the stratosphere–ionosphere coupling during stratospheric warmings. Geophysical Research Letters 39, L08101, http://dx.doi.org/10.1029/2012GL051261.

Groves, G.V., 1982. Hough components of ozone heating. Journal of Atmospheric and Terrestrial Physics 44, 111–121.

Gurubaran, S., Rajaram, R., 2000. Signatures of equatorial electrojet in the mesospheric partial reflection drifts over magnetic equator. Geophysical Research Letters 27, 943–946.

Hoffmann, P., Singer, W., Keuer, D., Hocking, W.K., Kunze, M.K., Murayama, Y., 2007. Latitudinal and longitudinal variability of mesospheric winds and temperature during stratospheric warming events. Journal of Atmospheric and Solar–Terrestrial Physics 69, 2355–2366.

Jacobi, Ch., et al., 1999. Climatology of the semidiurnal tide at 52–56°N from ground-based radar wind measurements 1985–1995. Journal of Atmospheric and Solar–Terrestrial Physics 61, 975–991.

Liu, H.-L., Wang, W., Richmond, A.D., Roble, R.G., 2010. Ionospheric variability due to planetary waves and tides for solar minimum conditions. Journal of Geophysical Research 115, A00G01, http://dx.doi.org/10.1029/2009JA015188.

Manney, G.L., et al., 2011. Unprecedented Arctic ozone loss in 2011. Nature 478 (46), 475, http://dx.doi.org/10.1038/nature10556.

McIntyre, M.E., 1982. How well do we understand the dynamics of stratospheric warmings? Jounal of Meteorological Society of Japan 60, 37–65.

Pancheva, D., Mukhtarov, P., Andonov, B., 2009. Nonmigrating tidal activity related to the sudden stratospheric warming in the Arctic winter of 2003/2004. Annales Geophysicae 27, 975–987.

Pedatella, N. M., Forbes, J. M., 2010. Evidence for stratosphere sudden warming-ionosphere coupling due to vertically propagating tides. Geophysical Research Letters 37, L11104, doi: http://dx.doi.org/10.1029/2010GL043560.

Rajaram, R., Gurubaran, S., 1998. Seasonal variabilities of low latitude mesospheric winds. Annales Geophysicae 16, 197–204.

Scheiben, D., Straub, C., Hocke, K., Forkman, P., Kampfer, N., 2011. Middle atmospheric water vapor and ozone anomalies during the 2010 major sudden stratospheric warming. Atmospheric Chemistry and Physics Discussions 11, 32391–32422 2011.

Scott, R.K., Polvani, L.M., 2004. Stratospheric control of upward wave flux near the tropopause. Geophysical Research Letters 31, L02115, http://dx.doi.org/10.1029/2003GL017965.

Smith, A.K., López-Puertas, M., Garcia-Comas, M., Tukiainen, S., 2009. Saber observations of mesospheric ozone during NH later winter 2002–2009. Geophysical Research Letters 36, L23804, http://dx.doi.org/10.1029/2009GL040942.

Sathishkumar, S., Sridharan, S., 2009. Planetary and gravity waves in the mesosphere and lower thermosphere region over Tirunelveli (8.7°N, 77.8°E) during stratospheric warming events. Geophysical Research Letters 36, L07806, http://dx.doi.org/10.1029/2008GL037081.

Sridharan, S., Sathishkumar, S., Gurubaran, S., 2012. Variabilities of mesospheric tides during sudden stratospheric warming events of 2006 and 2009 and their relationship with ozone and water vapour. Journal of Atmospheric Solar–Terrestrial Physics 78–79, 108–115, http://dx.doi.org/10.1016/j.jastp.2011.03.013, ISSN 1364-6826.

Sridharan, S., Sathishkumar, S., Gurubaran, S., 2009. Variabilities of mesospheric tides and equatorial electrojet strength during major stratospheric warming events. Annales Geophysicae 27, 4125–4130.

Stening, R.J., 2011. Lunar tide in the equatorial electrojet in relation to stratospheric warmings. Journal of Geophysical Research 116, A12315, http://dx.doi.org/10.1029/2011JA017047.

Stening, R.J., Meek, C.E., Manson, A.H., 1996. Upper atmosphere wind systems during reverse equatorial electrojet events. Geophysical Research Letters 23, 3243–3246, http://dx.doi.org/10.1029/96GL02611.

Wang, H., Fuller-Rowell, T.J., Akmaev, R.A., Hu, M., Kleist, D.T., Iredell, M.D., 2011. First simulations with a whole atmosphere data assimilation and forecast system: the January 2009 major sudden stratospheric warming. Journal of Geophysical Research 116, A12321, http://dx.doi.org/10.1029/2011JA017081.

Xu, J., Smith, A.K., Jiang, G., Yuan, W., Gao, H., 2012. Features of the seasonal variation of the semidiurnal, terdiurnal and 6-h components of ozone heating evaluated from Aura/MLS observations. Annales Geophysicae 30, 259–281.

Yue, X., Schreiner, W.S., Lei, J., Rocken, C., Hunt, D.C., Kuo, Y.-H., Wan, W., 2010. Global ionospheric response observed by COSMIC satellites during the January 2009 stratospheric sudden warming event. Journal of Geophysical Research 115, A00G09, http://dx.doi.org/10.1029/2010JA015466.